

The Infrared Phase of QCD and Anderson Localization

Ivan Horváth^{a,b,c,*}

^a*Nuclear Physics Institute CAS,*

Hlavní 130, 25068 Řež (Prague), Czech Republic

^b*Department of Physics and Astronomy, University of Kentucky,*

506 Library Drive, Lexington KY 40506, USA

^c*Department of Physics, The George Washington University,*

725 21st St. NW, Washington DC 20052, USA

E-mail: horvath@ujf.cas.cz

When Anderson localization entered the QCD landscape, it was almost immediately thought about in connection with thermal phases, namely as a factor in the chiral transition. However, recent developments revealed an additional structure that made Anderson-like features central to the genesis of the entirely new thermal phase: the IR phase. I will explain these developments.

The XVIth Quark Confinement and the Hadron Spectrum Conference (QCHSC24)

19-24 August, 2024

Cairns Convention Centre, Cairns, Queensland, Australia

*Speaker

1. Introduction

In this talk I will describe what is shaping up as a new case of fruitful cross-fertilization between elementary particle and condensed matter physics. On the former side it involves a recent unexpected finding of a new thermal regime in QCD [1–4], characterized by proliferation of deeply infrared ($0 \lesssim \lambda \ll T$) Dirac modes, by decoupling of the infrared physics (IR-bulk separation), and by scale invariant glue in the ensuing IR component. This new regime is known as the *IR phase* and is interesting not only due to the novel nature of its thermal state but also due to the fact that the associated change may be a true phase transition occurring at temperature T_{IR} ($200 \text{ MeV} < T_{\text{IR}} < 230 \text{ MeV}$) just above the known range of crossover temperatures.

On the other side of the above relationship is the time-honored phenomenon of Anderson localization, namely the exponential pinning of a quantum particle by virtue of spatial disorder [5, 6]. This effect had a deep impact on condensed matter physics and various applied areas but its potential role at the fundamental level, such as in the Standard Model of elementary particles, was barely considered in the literature. A fruitful remark [7] suggested that, at sufficiently high temperatures, thermal fluctuations in the strong sector (QCD) may induce localization of quark modes in low-lying parts of Dirac spectra. The associated loss of IR quark mobility then led to the suggestion that QCD chiral transition (massless limit), and by proxy the transition in real-world QCD, could be viewed as analogous to metal-to-insulator transition of Anderson type [8]. Such considerations gained some traction when localization in hot QCD started to be investigated more systematically and the Anderson-like mobility edge $\lambda_A > 0$ was identified¹ at sufficiently high temperatures [9, 10].

But contradictions soon appeared as well [2, 11]. To that end, note that the “insulating” nature of hot thermal state in metal-to-insulator scenario signifies the absence of long-distance ($\gtrsim 1/T$) physics. This was assumed to arise due to the infrared (IR) modes being localized at shorter scales, and due to the expected depletion of Dirac spectrum in this range. But the strong proliferation of deep-IR modes at high temperatures contrary to expectations [2], and their chiral polarization properties [11], suggested that IR physics is actually present, raising the possibility that metal-to-insulator scenario may not reflect some key aspects of QCD reality.

This developing discord became sharp once the evidence for IR phase was presented and its defining features were laid down [1]. In this original work it was already proposed that the mobility edge $\lambda_A > 0$ is crucial for IR-bulk separation, and that non-analyticity introduced by it shields the IR from renormalization-group running in line with the observed IR scale invariance. But the nature of the emerged IR physics remained foggy. The crucial step in this regard was taken in Ref. [3] which studied effective spatial dimensions of IR modes and, apart from intriguing non-analytic behavior (in λ) suggesting topology at play, found that point $\lambda_{\text{IR}} \equiv 0$ behaves in certain regards similarly to the mobility edge λ_A . Ref. [4] then provided evidence that λ_{IR} is indeed a new Anderson-like mobility edge, and formulated the *metal-to-critical* scenario of transition to IR phase based on both edges.

The metal-to-critical scenario is conveyed by the phase diagram for Anderson-like properties of thermal QCD [4], shown in Fig. 1. Here the thick red lines in λ – T plane represent the Anderson-like critical points (mobility edges). Dashing at the horizontal segment $T = T_{\text{IR}}$ signifies that it may be of zero length (single point), and dashing at $T = T_{\text{UV}}$ conveys that T_{UV} may be infinite. In IR phase,

¹Note that in this continuum notation, where non-zero Dirac eigenvalues come in conjugate pairs $\pm i\lambda$, we frequently only consider the upper branch $\lambda \geq 0$.

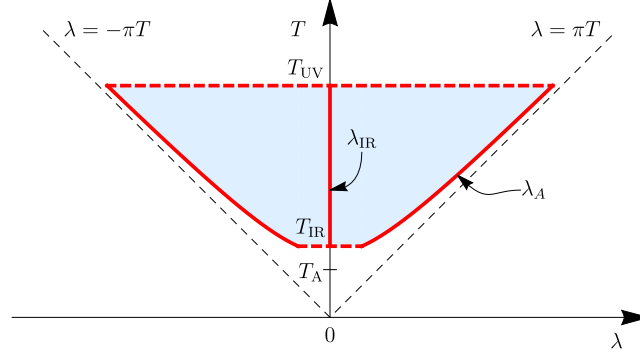


Figure 1: Phase diagram for Anderson-like properties in the Dirac spectrum of thermal QCD [4]. See the explanation in the text. Temperature T_A is the crossover point for Dirac spectral properties [1] and thin dashed lines represent the Matsubara scales.

namely for $T_{\text{IR}} < T < T_{\text{UV}}$, there are critical points $\pm\lambda_A$ and λ_{IR} in the Dirac spectrum, yielding the modes in the range $(-\lambda_A, \lambda_{\text{IR}}) \cup (\lambda_{\text{IR}}, \lambda_A)$ (the blue region) localized with varying localization lengths that diverge at $\pm\lambda_A$ and λ_{IR} . The chief tenet of the relationship between the thermal state of QCD in IR phase and its Anderson-like representation (metal-to-critical picture) is that the above constellation of critical points captures the unusual features found in the former: the non-analyticity at λ_A facilitates the IR-bulk separation and shields the IR from renormalization-group running, while the criticality at λ_{IR} determines the nature of its long-range physics.

In this talk I will describe in some detail the developments that led to the current notion of IR phase and emphasize, in particular, the role of Anderson localization ideas in that process.

2. IR Phase

Initial key steps toward the notion of IR phase were taken in Ref. [2]. The authors argued that a qualitatively new regime characterized by anomalously strong accumulation of IR Dirac modes exists in SU(3) gauge theories with fundamental quarks. They showed that this accumulation, observed in lattice-regularized theory, persists into the continuum limit and suggested that the ensuing IR degrees of freedom (dof's) decouple and defy confinement in this “partially deconfined” phase.

The proliferation of IR dof's remained the chief qualitative underpinning of the new regime but the concept of IR phase arose later with the revelation [1] that the effect is quantitatively expressed as a power-law (negative power) IR behavior of Dirac spectral density². In fact, at least in thermal cases, the near-pure power $p = -1 + \delta$ with very small $\delta \geq 0$ was found. All basic tenets of IR phase were formulated in that work, and SU(3) gauge theories with fundamental quarks were classified into three types (phases) based on a degree of their Dirac mode accumulation in deep IR, namely [1]

$$\rho(\lambda) \propto \lambda^p, \lambda \rightarrow 0 \quad \Rightarrow \quad \text{phase} = \text{B if } p = 0, \text{ IR if } p < 0, \text{ UV if } p > 0 \quad (1)$$

The names of phases are derived from the proposed relationship of IR glue to scale invariance: B is a shorthand for IR-Broken and corresponds to hadronic phase such as in real-world QCD at

²Recall that Dirac spectral density $\rho(\lambda)$ of the theory is the average number of Dirac eigenmodes per unit 4-volume and unit spectral interval in the infinitesimal neighborhood of λ .

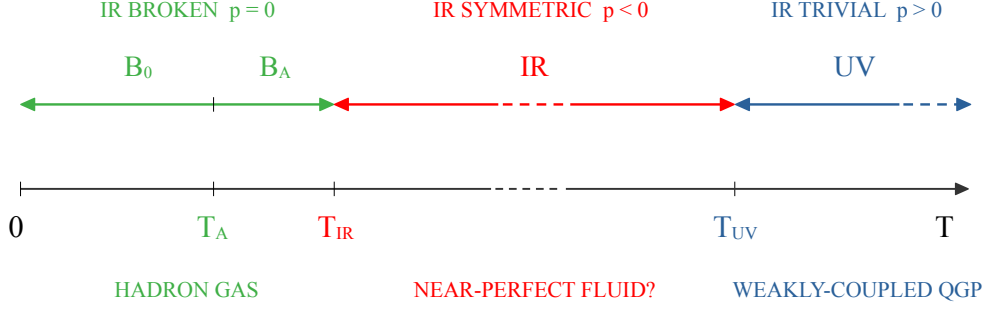


Figure 2: Types of phases in SU(3) gauge theories with fundamental quarks based on the abundance of deep-IR degrees of freedom and IR scale invariance. See the discussion in the text.

low temperatures.³ IR refers to the IR-Symmetric phase which is synonymous to the IR phase and for which a possible connection to near-perfect fluid medium observed at RHIC and LHC was raised [1]. UV dubs “IR-Trivial” since IR degrees of freedom are power-law suppressed. This regime would correspond to weakly-coupled quark-gluon plasma. Note that the nominal expectation is that $\rho(\lambda) \propto \lambda^3$ in UV ($\lambda \rightarrow \infty$) for all three phases due to asymptotic freedom.

The above is schematically represented by Fig. 2. The order from left-to-right follows the case when transitions are induced by increasing temperature. Temperature T_A marks a generic crossover in Dirac spectral properties. This transition is thus on the same footing as the chiral or other crossovers. Temperatures T_{IR} and T_{UV} mark transitions to IR and UV phases respectively.

The phase structure in the full set \mathcal{T} of SU(3) gauge theories with fundamental quarks is shown schematically in Fig. 3 (left) [2]. \mathcal{T} is a multidimensional space (T , number of flavors N_f , individual quark masses) and only T and N_f have an explicit representation in Fig. 3 (left). The accumulated knowledge endowing the scheme with information is that the phase sequence $B \rightarrow IR \rightarrow UV$ (or any part of it) occurs not only via increasing the temperature, but also via increasing the number of flavors and via *decreasing* the individual quark masses m_i [1]. Important case is when IR phase arises from B phase at sufficiently large N_f by lowering the quark masses alone. In

³Note that the logarithmic IR behaviors, such as one predicted in low-temperature QCD by chiral perturbation theory [12], entail $p=0$ and belong to B phase.

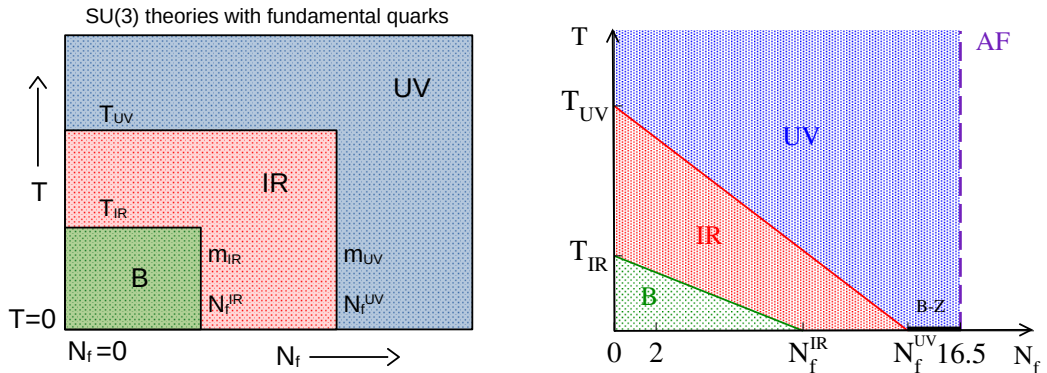


Figure 3: Left: schematic phase diagram of SU(3) gauge theories with fundamental quarks (set \mathcal{T}) based on the abundance of deep-IR degrees of freedom and IR scale invariance. Right: the case of near-massless quarks. The asymptotic freedom (AF) boundary is at $N_f=16.5$. See the discussion in the text.

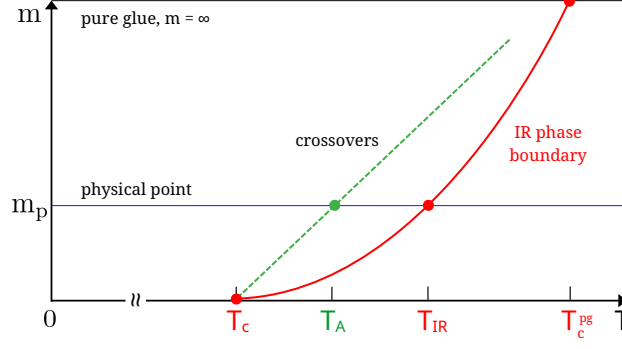


Figure 4: The conjectured $N_f = 2$ (or $N_f = 2 + 1$) thermal QCD phase diagram including the IR phase [1]. See e.g. the talk by I. Horváth at FunQCD22 workshop for one of the explicit mentions of this structure: https://drive.google.com/file/d/1vZ0AY0WsZAf9iV7-Br-E_2NiwaZzRGp/view.

the degenerate near-massless case this situation is schematically shown in Fig. 3 (right), which for $T \rightarrow 0$ approaches what is known as the conformal window region [13]. The corresponding transition parameters N_f^{IR} and N_f^{UV} delimit its strongly-coupled part [1] while theories in the regime $(N_f^{\text{UV}}, 16.5)$ are expected to be governed by the weakly-coupled Banks-Zaks fixed point. Note that the straight-line phase boundaries in Fig. 3 signify the lack of more detailed knowledge at present.

The important special case is the T – m phase diagram for $N_f = 2$ (mass-degenerate) flavors or for $N_f = 2 + 1$ flavors with heavy quark at the physical strange-quark mass. These are both very accurate representations of “real-world QCD” when light-quark mass m is set to physical value. Varying m probes the effects of light quarks and the approach to the chiral limit. The simplest scenario with IR phase included is shown in Fig. 4. IR phase transitions are traced by the red line starting at $m = 0$ with the chiral transition at T_c , passing through T_{IR} at the physical point, and ending at the Polyakov-line transition of pure-gluon theory ($m = \infty$) denoted as T_c^{pg} . Generic crossovers (e.g. the chiral one) are represented by the green dashed line, with T_A denoting their temperature.

2.1 Some Key Evidences

The power of numerical lattice QCD lies, among other things, in the fact that by virtue of fully realizing a regularized system, it can verify its conjectured features. By the same token, it can also discover qualitatively new aspects that were not even considered. IR phase is an example of this. Indeed, it was widely expected that thermal fluctuations universally suppress IR dof’s and Dirac spectrum was generally assumed to become IR-depleted upon the “QCD transition”. Instead, Fig. 5 shows the state of the art results for spectral densities of the overlap Dirac operator in pure-gluon (left) and real-world (right) QCD, with an entirely different IR world clearly emerging at large volumes.

Two ingredients were of key relevance for the notion of IR phase to develop. The first one relates to the generic worry that lattice observations may be regularization artifacts that disappear in the continuum limit. This was resolved for pure-gluon QCD in Ref. [2] and for “real-world” QCD ($N_f = 2 + 1$ at physical point) in Ref. [16]. Fig. 6 shows the UV cutoff dependences of mode abundance in the inner core of the IR peak which reliably extrapolate to non-zero values.

The second key ingredient was the revelation that the unusual IR accumulation has a power-law character [1]. In particular, $\rho(\lambda)$ behaves in IR as a near-pure power λ^p with $p = -1 + \delta$ and $\delta > 0$ very small. This is shown in Fig. 7 where the variables were chosen so that pure $p = -1$ corresponds to a rising straight line. In particular, $\sigma(\lambda, T)$ is a cumulative density for the interval

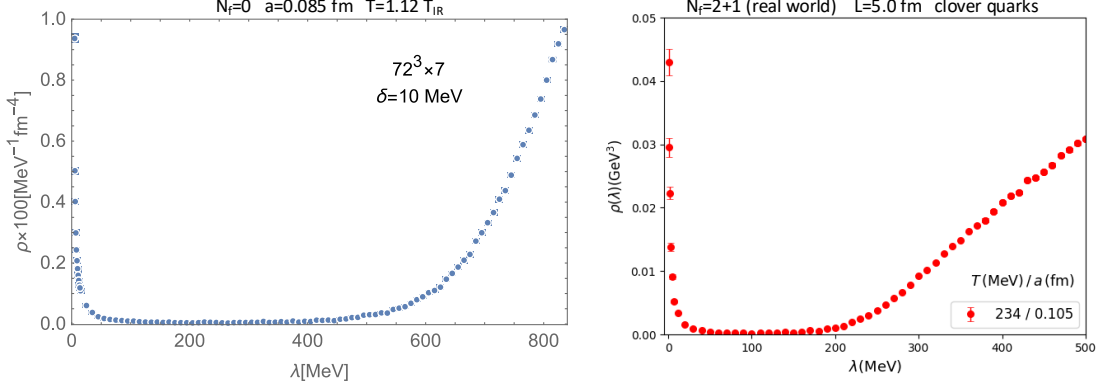


Figure 5: Dirac spectral densities for pure-gluon QCD (left, [14]) and “real-world” ($N_f = 2 + 1$) QCD (right, [15]) in IR phase. The parameters of regularized systems in question are specified in the plots.

(λ, T) . Approaching deeper IR means moving to the right on the plots. Notice that in pure-gluon case the drastic change occurs when changing $T = 0.98 T_{\text{IR}}$ to $T = 1.12 T_{\text{IR}}$ and the power law in IR phase persists for over three orders of magnitude in scale. Temperature T_{IR} coincides with T_c of the Polyakov line transition [1]. The “real-world” case behaves very similarly at $T = 250 \text{ MeV}$, although the range of power law is smaller due to smaller volumes.

2.2 Why IR and Why Phase?

The “IR” in IR phase arose from the qualitatively enhanced propensity of dof’s to be arbitrarily infrareded upon crossing into this new regime. The connection to IR fixed points associated with the conformal window offered itself naturally [1] although the details still need to be investigated. Most of the concluded features of the phase come from studies of thermal QCD with temperature being the transition-inducing parameter. From the physics standpoint, this is arguably the most important setting to investigate in fact. At present, the best estimate for the value of T_{IR} in real-world QCD comes from $N_f = 2 + 1$ studies at physical quark masses and yield [1, 15, 16]

$$200 \text{ MeV} < T_{\text{IR}} < 230 \text{ MeV} \quad (2)$$

Note that the well-known chiral crossover temperature is $T_A \rightarrow T_A^c \approx 155 \text{ MeV}$ [17–19].

Several intriguing proposed features of the IR regime make it a phase in the conventional sense [1, 3, 4]. In particular, upon crossing into the IR phase the following occurs:

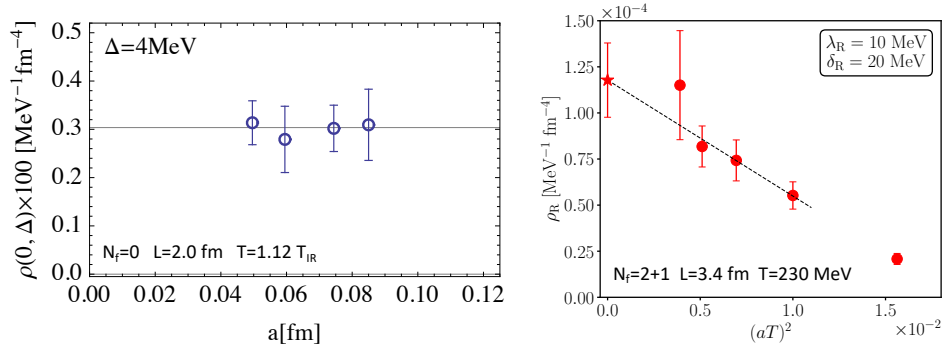


Figure 6: Scaling of the strength of IR peak in Dirac spectral densities for pure-gluon QCD (left, overlap, [2]) and “real-world” QCD (right, staggered, [16]). The latter uses staggered dynamical lattice quarks.

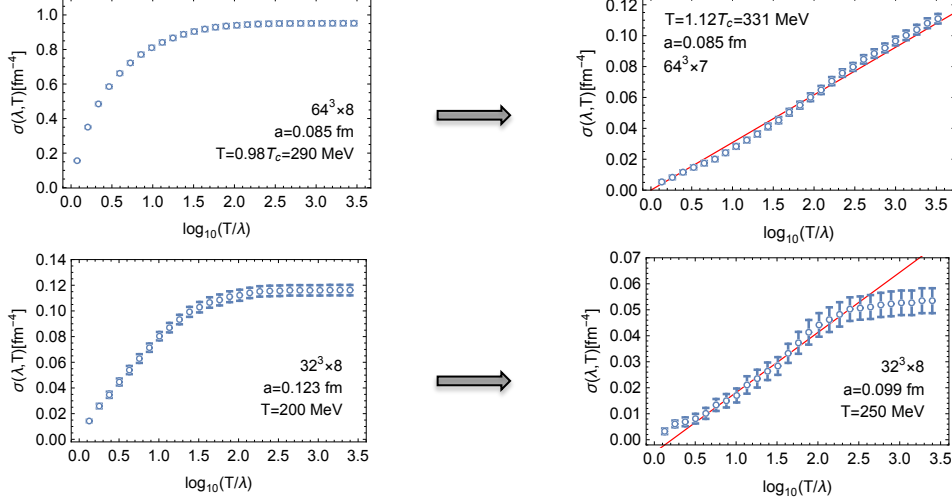


Figure 7: Transitions to IR phase in pure-glue (top) and “real-world” QCD (bottom) [1]. See the explanation in the text. Real-world QCD refers to $N_f = 2 + 1$ at the physical point.

- (i) **IR-Bulk Separation.** The system becomes multicomponent with the IR segment decoupling and becoming an autonomous subsystem (independent component).
- (ii) **IR Scale Invariance.** Glue fields of the IR component become scale invariant (at least asymptotically in IR).
- (iii) **Non-Analyticity.** Non-analytic behavior in Dirac spectral properties (in λ -dependence) appears and translates into non-analytic T -dependence of physical observables at the transition.
- (iv) **Infinite Glue Screening Lengths.** Gluon fields start exhibiting long-range spatial correlations.

In the following section we will describe how these features interrelate with the existence of Anderson-like transitions in high-temperature QCD.

3. IR Phase and Anderson-like Localization

At the time the notion of IR phase was put forward in [1], some of the arguments for justification of properties (i)-(iv) already utilized the existence of the Anderson-like mobility edge $\lambda_A > 0$ in Dirac spectra at high temperatures. When the metal-to-critical scenario utilizing also the new mobility edge at $\lambda_{\text{IR}} = 0$ was put forward [3, 4] (see Sec. 1), essentially all proposed features of IR phase could be thought about under that umbrella. In this section we describe this ensuing relationship between the Anderson-like localization phenomena and thermal QCD.

3.1 Anderson Mobility Edges

Anderson localization is an old subject [5] that became quite vast in part due to the wealth of its applications [6]. For present purposes we only need a cursory knowledge of the topic, mostly embodied in the abstract notion of Anderson transitions or the associated critical points: the mobility edges. On one side of the transition are extended (“conducting”) states while on the other side the exponentially localized (“insulating”) ones. Transition occurs due to spatial disorder (e.g. random potentials), and the criticality at the edge is conveyed, among other things, by the

fact that the density-density (probability-probability) spatial correlation length in modes diverges. Schematics of these transitions are shown in Fig. 8. For example, when approaching the mobility edge indicated by energy $E_{c1} > 0$ on the phase diagram (left plot) from the localized side $E > E_{c1}$, then the geometric scale ℓ (mode size, “localization length”) associated with the mode varies as

$$\ell(E) \propto (E - E_{c1})^{-\nu} \propto \xi(E) \quad \nu > 0 \quad (3)$$

and is proportional to the correlation length ξ . Directly at criticality, the density-density correlation function becomes long-range namely $L^6 \langle p(r)p(r') \rangle \propto (|r - r'|/L)^{-\eta}$ in 3D (see e.g. [21]). Here $p(r) = \psi^\dagger \psi(r)$ with ψ the eigenstate.

3.2 IR-Bulk Separation

The idea of IR-Bulk separation became suggestive after the striking bimodal structure of spectral densities became the fact of the continuum limit [2]. However, that in itself doesn’t guarantee that the modes, and thus the physics itself, associated with spectral segments so separated are fully independent of one-another. One possibility that would make this very assuring is e.g. if $\rho(\lambda)$ had a region of full depletion ($\rho = 0$) between the two parts. While it is very possible that this does happen upon removing both the IR and UV cutoffs, it has not been verified in simulations yet.

But it is also not necessary. Indeed, there may be a large class of other spectral non-analyticities separating IR and Bulk that indicate their decoupling. To that end, the original work [1] suggested that Anderson-like mobility edge $\lambda_A > 0$ [9, 10] fits the bill in terms of providing for the needed non-analytic setup. Indeed, it is a critical point (internal “phase transition”) within the Dirac substructure of QCD, and modes below and above λ_A are thus not expected to talk to each other. In fact, if λ_A is truly Anderson-like then spatial correlations across this edge explicitly conform to that [6]. Thus, in the metal-to-critical picture of IR phase transition, IR-bulk separation is produced via λ_A .

3.3 IR Scale Invariance and Infinite Glue Screening Lengths

The chief initial motivation for IR scale invariance in IR phase [1] was the near-pure power-law behavior of $\rho(\lambda)$: in the spirit of the inverse scattering problem in quantum mechanics, this was suggested to be the result of scale invariance (in the statistical sense) of the underlying glue. Another motivation was that similar IR accumulation of Dirac modes also occurs in the vicinity of conformal window ($T=0$) as a result of lowering quark masses [11, 22]. This then suggested the contiguous IR phase region in the theory space (Fig. 3) and made IR scale invariance natural in that sense.

The metal-to-critical scenario of transition to IR phase associates the appearance of long-range correlations (power-law decays; infinite correlation lengths) with the formation of strictly

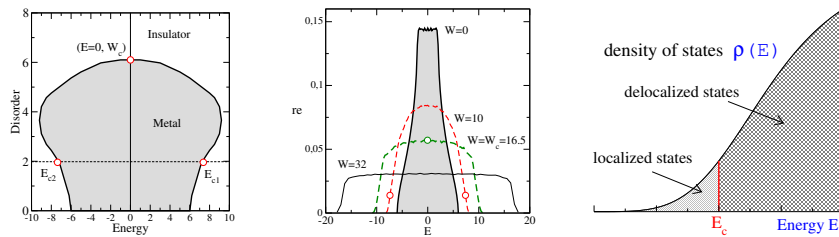


Figure 8: Generic schematics of Anderson transitions: phase diagram, density of states and the mobility edge. Courtesy of Peter Markoš and Ref. [20].

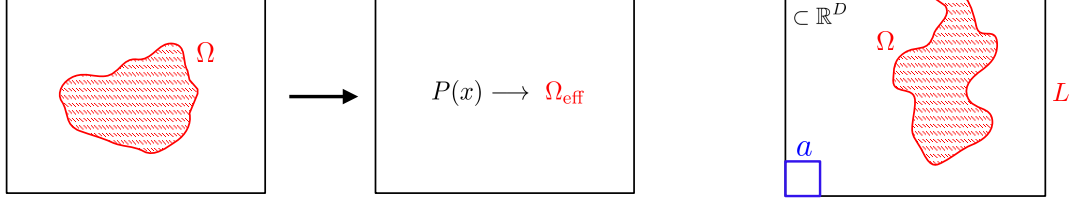


Figure 9: Left: Instead of the fixed subset Ω and its measure, Effective-Number Theory shows how to define the effective subset Ω_{eff} from the underlying probability distribution $P(x)$. Right: IR dimension quantifies the change in the measure of the set Ω (or Ω_{eff}) in response to change of IR cutoff L .

IR Anderson-like mobility edge $\lambda_A = 0$ upon crossing T_{IR} [3, 4]. Indeed, identifying the IR phase transition with the emergence of λ_A means that critical correlations in deep-IR Dirac modes ensue upon entering the phase. This, in turn, translates into long-range correlations in gluonic composite fields which can be scale-decomposed in terms of these eigenmodes [23–25].

Metal-to-critical scenario thus not only incorporates infinite glue screening lengths and (at least an asymptotic) IR scale invariance of glue in the IR phase, but also provides for a concrete and from the particle physics point of view highly unusual mechanism of their origin.

3.4 Non-Analyticity

Phase transitions are characterized by non-analytic behavior of observables in thermodynamic limit. Identification of such non-analyticities in transitions to IR phase went hand-in-hand with formulation of the metal-to-critical picture [3, 4]. Indeed, dramatic feature of Anderson transitions is the spatial dimensional collapse of states on the localized side. Given the presence of Anderson-like mobility edges in IR phase, this aspect became intuitively connected to roots of non-analyticity. But formalization of dimensional arguments turned out to be a non-trivial task. Indeed, the notion of spatial dimension associated with Schrödinger states (or with probability distributions in metric spaces more generally) didn't exist in the usual measure-based Hausdorff/Minkowski sense. This was rectified by the Effective-Number Theory [26] which constructed the needed effective counting measures (Fig. 9 left), and subsequently by the Effective-Dimension Theory [27] which showed that these measures lead to the unique notion of effective dimension.

Rather than UV dimension familiar from analyses of fractal sets, it is the unconventional IR dimension [27] that is of prime interest here. While UV dimension gauges the response of set measure to the decrease of UV cutoff a , IR dimension probes the increase of IR cutoff L , namely

$$N_+(\Omega, a, L) \propto L^{d_{\text{IR}}(\Omega, a)} \quad \text{or} \quad \mathcal{N}_\star(P, a, L) \propto L^{d_{\text{IR}}(P, a)} \quad \text{for} \quad L \rightarrow \infty \quad (4)$$

for fixed sets and probability distributions respectively [27]. Here N_+ is the number of elementary

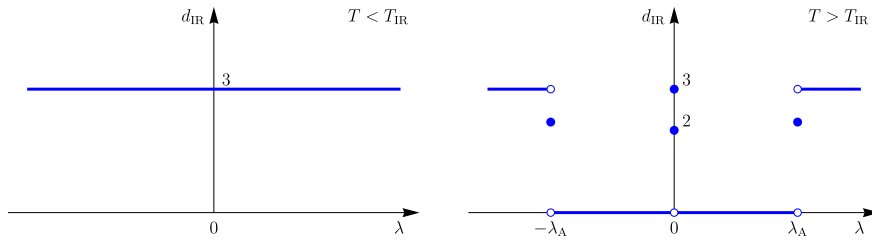


Figure 10: IR dimensions of QCD Dirac modes in the B phase (left) and in the IR phase (right) [28].

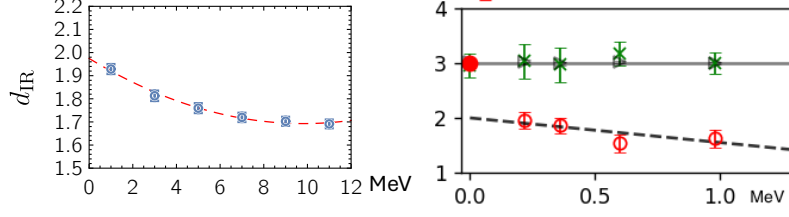


Figure 11: IR dimensions of near-zero (critical) modes in IR phase. On the x-axis is the width of the near-zero region. Left [3]: pure-gluon QCD at $T = 0.12T_{\text{IR}}$. Right [15]: $N_f = 2 + 1$ real-world QCD at $T = 234$ MeV (red) and at $T = 187$ MeV (green, outside of IR phase). Full symbols are exact zeromodes.

volume elements covering Ω at given a and L , while \mathcal{N}_\star is the minimal effective count [26] of these elements given the $P(x)$ in question. Schematics of this is shown in the right plot of Fig. 9.

For Dirac modes of QCD and Schrödinger states of Anderson models, IR dimension is a function of Dirac scale (λ) or energy (E), and $P(x)$ is encoded by modes/states. Effective counts \mathcal{N}_\star on which d_{IR} is based are QCD/disorder averaged. Extensive calculations [3, 15, 28] support the spectral portrait of IR dimensions in QCD shown schematically in Fig. 10. While $d_{\text{IR}} = 3$ across the Dirac spectrum for $T < T_{\text{IR}}$, in IR phase there is a pattern of discontinuities at mobility edges $\pm\lambda_A$ and $\lambda_{\text{IR}} = 0$. Intriguing aspect is that exact zeromodes have $d_{\text{IR}} = 3$, but the lowest near-zero (critical) modes have $d_{\text{IR}} = 2$. The relevant evidence for this is shown in Fig. 11 for both the pure-gluon [3] and the $N_f = 2 + 1$ real-world QCD [15]. In the latter case the data nicely distinguishes the thermal state at $T = 187$ MeV, which is not in IR phase, from that at $T = 234$ MeV which is inside the phase.

Given the singular accumulation of near-zero modes in IR phase, $d_{\text{IR}} = 2$ dominates its deep-IR physics: non-analyticity of $\rho(\lambda)$ leads to non-analyticity of observables at $T = T_{\text{IR}}$. For example, the above results imply $d_{\text{IR}}(T)$ for the IR part of action density shown in Fig. 12 (See Refs. [23–25]).

4. Conclusions

The chief purpose of this talk is to convey that, by virtue of the new IR phase, Anderson-like localization found a relevant place in the Standard Model of particle physics [4]. While a precise relation between “Anderson and Anderson-like” is yet to be determined, it is clear that the ideas developed in the former context are very fruitful for building a detailed understanding of the recently uncovered IR regime represented by the IR phase.⁴

Acknowledgments

I greatly acknowledge the long-term productive collaboration with Andrei Alexandru and the extensive technical help from Dimitris Petrellis. Hali, Sylvia and Vlado made this text possible.

References

- [1] Andrei Alexandru and Ivan Horváth. Possible New Phase of Thermal QCD. *Phys. Rev. D*, 100(9):094507, 2019.
- [2] Andrei Alexandru and Ivan Horváth. Phases of SU(3) Gauge Theories with Fundamental Quarks via Dirac Spectral Density. *Phys. Rev.*, D92(4):045038, 2015.

⁴ I wish to acknowledge few additional works [29–32] related in various ways to the developments described here.

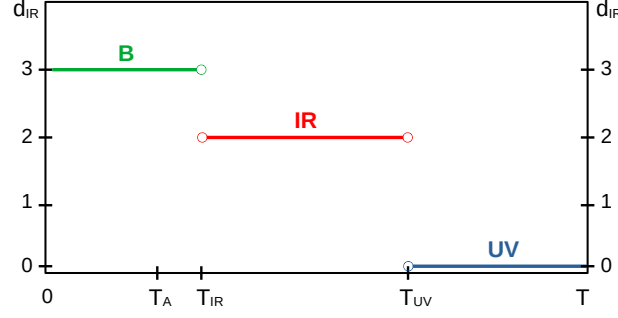


Figure 12: T-dependence of d_{IR} for deep-IR Dirac modes which is also the spatial dimension of IR part in F^2 .

- [3] Andrei Alexandru and Ivan Horváth. Unusual Features of QCD Low-Energy Modes in the Infrared Phase. *Phys. Rev. Lett.*, 127(5):052303, 2021.
- [4] Andrei Alexandru and Ivan Horváth. Anderson metal-to-critical transition in QCD. *Phys. Lett. B*, 833:137370, 2022.
- [5] P. W. Anderson. Absence of diffusion in certain random lattices. *Phys. Rev.*, 109:1492–1505, Mar 1958.
- [6] Elihu Abrahams. *50 Years of Anderson Localization*. WORLD SCIENTIFIC, 2010.
- [7] Adam Miklos Halasz and J. J. M. Verbaarschot. Universal fluctuations in spectra of the lattice Dirac operator. *Phys. Rev. Lett.*, 74:3920–3923, 1995.
- [8] Antonio M. Garcia-Garcia and James C. Osborn. Chiral phase transition in lattice QCD as a metal-insulator transition. *Phys. Rev. D*, 75:034503, 2007.
- [9] Tamas G. Kovacs and Ferenc Pittler. Anderson Localization in Quark-Gluon Plasma. *Phys. Rev. Lett.*, 105:192001, 2010.
- [10] Matteo Giordano, Tamas G. Kovacs, and Ferenc Pittler. Universality and the QCD Anderson Transition. *Phys. Rev. Lett.*, 112(10):102002, 2014.
- [11] Andrei Alexandru and Ivan Horváth. Chiral Symmetry Breaking and Chiral Polarization: Tests for Finite Temperature and Many Flavors. *Nucl. Phys.*, B891:1–41, 2015.
- [12] J. C. Osborn, D. Toublan, and J. J. M. Verbaarschot. From chiral random matrix theory to chiral perturbation theory. *Nucl. Phys.*, B540:317–344, 1999.
- [13] Tom Banks and A. Zaks. On the Phase Structure of Vector-Like Gauge Theories with Massless Fermions. *Nucl. Phys.*, B196:189–204, 1982.
- [14] Andrei Alexandru and Ivan Horváth. 2023, unpublished.
- [15] Xiao-Lan Meng, Peng Sun, Andrei Alexandru, Ivan Horváth, Keh-Fei Liu, Gen Wang, and Yi-Bo Yang. Separation of Infrared and Bulk in Thermal QCD. *JHEP*, 2024(12):101, 2024.
- [16] Andrei Alexandru, Claudio Bonanno, Massimo D’Elia, and Ivan Horváth. Dirac spectral density in $N_f=2+1$ QCD at $T=230$ MeV. *Phys. Rev. D*, 110(7):074515, 2024.

- [17] Y. Aoki, G. Endrodi, Z. Fodor, S.D. Katz, and K.K. Szabo. The Order of the quantum chromodynamics transition predicted by the standard model of particle physics. *Nature*, 443:675–678, 2006.
- [18] Y. Aoki, Szabolcs Borsanyi, Stephan Durr, Zoltan Fodor, Sandor D. Katz, Stefan Krieg, and Kalman K. Szabo. The QCD transition temperature: results with physical masses in the continuum limit II. *JHEP*, 06:088, 2009.
- [19] A. Bazavov et al. Chiral crossover in QCD at zero and non-zero chemical potentials. *Phys. Lett. B*, 795:15–21, 2019.
- [20] P. Markoš. Numerical analysis of the anderson localization. *Acta Physica Slovaca*, 56(5):561–685, Oct 2006.
- [21] Ferdinand Evers and Alexander D. Mirlin. Anderson transitions. *Reviews of Modern Physics*, 80(4):1355–1417, Oct 2008.
- [22] Andrei Alexandru, Ivan Horváth. Broken Valence Chiral Symmetry and Chiral Polarization of Dirac Spectrum in $N_f=12$ QCD at Small Quark Mass. *AIP Conf. Proc.*, 1701(1):030008, 2016.
- [23] Ivan Horváth. Coherent lattice QCD. *PoS*, LAT2006:053, 2006.
- [24] Ivan Horváth. A Framework for Systematic Study of QCD Vacuum Structure II: Coherent Lattice QCD. *arXiv:hep-lat/0607031*, 2006.
- [25] Andrei Alexandru, Ivan Horváth, and Keh-Fei Liu. Classical Limits of Scalar and Tensor Gauge Operators Based on the Overlap Dirac Matrix. *Phys.Rev.*, D78:085002, 2008.
- [26] Ivan Horváth and Robert Mendris. Effective Number Theory: Counting the Identities of a Quantum State. *Entropy*, 22:1273, 2020.
- [27] Ivan Horváth, Peter Markoš, and Robert Mendris. Counting-Based Effective Dimension and Discrete Regularizations. *Entropy*, 25(3):482, 2023.
- [28] Andrei Alexandru, Ivan Horváth, and Neel Bhattacharyya. Localized modes in the IR phase of QCD. *Phys. Rev. D*, 109(1):014501, 2024.
- [29] Robert G. Edwards, Urs M. Heller, Joe E. Kiskis, and Rajamani Narayanan. Chiral condensate in the deconfined phase of quenched gauge theories. *Phys.Rev.*, D61:074504, 2000.
- [30] Viktor Dick, Frithjof Karsch, Edwin Laermann, Swagato Mukherjee, and Sayantan Sharma. Microscopic origin of $U_A(1)$ symmetry violation in the high temperature phase of QCD. *Phys. Rev.*, D91(9):094504, 2015.
- [31] Robin Kehr, Dominik Smith, and Lorenz von Smekal. QCD Anderson transition with overlap valence quarks on a twisted-mass sea. *Phys. Rev. D*, 109(7):074512, 2024.
- [32] Tamas G. Kovacs. Fate of Chiral Symmetries in the Quark-Gluon Plasma from an Instanton-Based Random Matrix Model of QCD. *Phys. Rev. Lett.*, 132(13):131902, 2024.